Mathematical modelling of a hybrid solar entrained-flow gasifier

P.J. van Eyk[1, *], P.J. Ashman[1] and G.J. Nathan[2]

Centre for Energy Technology, Schools of [1]Chemical Engineering and [2]Mechanical Engineering

The University of Adelaide, South Australia 5005, Australia

Abstract

   A 1-dimensional mathematical model has been developed for a hybrid solar entrained-flow gasifier that includes the effects of both high intensity solar radiation (during peak sun) and oxygen blown gasification (during high cloud cover or at night). Calculations using this model predict that solar gasification of Illinois 6 coal during peak sun will result in similar coal conversions (~95%), higher H_2/CO ratios (1.5 cf 0.37) and lower CO_2 concentrations of the syngas (2% cf 7% at the exit) relative to oxygen blown gasification. Due to these large differences in outlet composition, it is apparent that syngas storage is necessary for a coal to liquids plant with a hybrid solar/oxygen entrained-flow gasifier.

Keywords: Solar, gasification, coal, model.

1. Introduction

Solar gasification of carbonaceous feedstocks is a process that makes use of concentrated solar energy to convert a solid fuel, such as coal or biomass, into a high-quality synthesis gas (syngas), comprised mainly of H_2 and CO, which can then be converted via available processes (e.g. Fischer–Tropsch synthesis) to yield a high-value synthetic transport fuel. Synthetic fuels produced using this technology would have a much lower carbon footprint than conventional alternatives [1]. Solar gasification reactors have been under investigation since the 1980s. A wide range of solar reactors have been examined, including packed-bed [2], fluidised-bed [3] and entrained-flow gasifiers [4]. Recently, an innovative design that couples entrained flow gasification with direct solar irradiation has been proposed and experimentally demonstrated, termed the solar vortex reactor [4]. The technical viability of this windowed reactor to gasify petroleum coke (pet coke) has been demonstrated at atmospheric pressure at small scale. Furthermore, the similarity of this device to vortex combustors suggests that it is well suited to being adapted to operate as a hybrid device. In such a hybrid device the endothermic demand of the gasification process is proposed to be met by solar energy (when available) and/or by oxy-fuel combustion of coal when solar insolation is insufficient – e.g. during periods of high cloud cover or at night. However, the potential of the vortex reactor to operate successfully as a hybrid reactor is yet to be evaluated. Hence, there is a need for an evaluation of entrained-flow solar gasification with varying solar fluxes and oxygen flows.

Preliminary numerical modelling of the vortex reactor by Z'Graggen *et al.* [5], has shown that the temperature distribution and overall carbon conversions within the gasifier can be predicted with reasonable accuracy. However, the use of pet coke as a feedstock avoided the need to consider several issues that become important for entrained-flow solar gasification of more common carbonaceous feedstocks, such as coal and biomass. The pet coke fuel used in previous experimental [4] and modelling [5] studies has a low content of both volatiles and ash, relative to most other fuels. Char gasification reactivities, are also expected to differ significantly between petroleum coke and more typical gasification feedstocks. Hence the gasification of fuels such as coal and biomass with solar energy will require the need to model the effects of radiation on devolatilisation and char reactions. This challenge is particularly significant in the solar vortex reactor which employs direct radiative heat transfer, owing to its extremely high fluxes, which also make it much more efficient than indirect heat transfer devices. Importantly, the heat fluxes due to direct solar radiation are potentially higher than those usually considered for radiative heat transfer in previous gasification studies. Additionally, it is expected that the outlet syngas composition will be affected by the use of solar energy during sunlight hours. However, the extent of these variations and the possible impact on the downstream processes is unclear. Hence there is a need to better understand the influence of high flux radiation on the gasification behavior of coal and biomass by developing more complete models than those established previously [5].

The overall aim of this paper is therefore to develop a mathematical model of an entrained-flow gasifier that includes intense solar radiation coupled with coal gasification. The model is based on existing entrained-flow gasifier models that have been developed for coal gasification [6]-[7], but is extended to include intense solar radiation.

2. Model development

2.1 Model Description and assumptions

The influence of high flux radiation on the gasification of coal is assessed in the simplified environment of a 1-D entrained-flow gasifier. The reactor is modelled as a plug flow reactor and is shown schematically in Figure 1. Each slice along the reactor was treated as a perfectly mixed zone of particles and

---

* Corresponding author:

Phone: (+61) 8 83035056

Email: philip.vaneyk@adelaide.edu.au

gas. The particles were assumed to have the same axial velocity as the gas in each zone, and zero radial velocity.

Solar energy is assumed to enter the reactor axially through a window and in the same direction as the gas and solid flows. The influence of particles on the propagation of radiation is included by utilizing the absorbtivity data calculated by Z'Graggen *et al.* for particles in the vortex reactor [5]. The fuel chosen for the study was Illinois 6 coal, the properties of which are given in Table I. The coal particles were assumed to be 100μm in diameter. Due to the small particle size, the temperature distribution within each particle was assumed as uniform for any instant in time.

A time step of 10^{-5} s was chosen to obtain an adequate convergence of the computational model described in Sections 2.2-2.6.
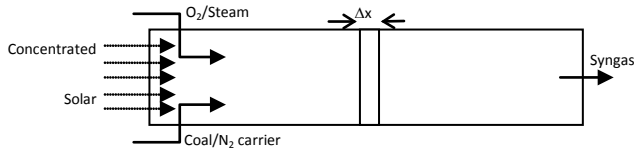

Table I: Proximate and ultimate analyses of the 'Illinois 6 coal' together with the modelled composition of the coal.

Proximate analysis	wt %	Modelled composition	wt %
Moisture	11.12	CO	12.08
Ash	9.7	H_2	0
Volatile matter	34.99	CO_2	0
Fixed carbon	44.19	CH_4	17.40
LHV (MJ/kg)	26.15	H_2O (l)	11.12
Ultimate analysis	**wt % db**	N_2	1.26
Carbon	71.72	C	45.77
Hydrogen	5.06	O_2	0
Oxygen	7.75	H_2S	2.67
Nitrogen	1.41	Ash	9.7
Sulfur	2.82	LHV (MJ/kg)	25.4
Ash	10.91		

2.2 Devolatilisation

Devolatilisation of coal was assumed to occur via reaction R1.

Coal → Char (C) + Volatiles (CO + CO_2 + H_2
$\qquad\qquad$ + H_2O + CH_4 + N_2 + H_2S) $\qquad$ (R1)
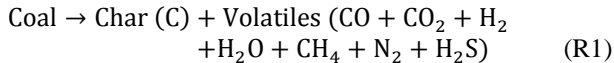
For the 'Illinois 6' design coal, a model coal composition is used to approximate the features of the real fuel. Fixed carbon was approximated by solid carbon, while the volatile matter is assumed to be released as a mixture of gases CH_4, CO, CO_2, H_2, H_2O, N_2, H_2S and HCl. The quantity of each of these gases released as volatiles was determined by balancing the elements present in coal from the ultimate analysis with the modelled composition, by obtaining as close as possible model char and volatile yields as those shown in the proximite analysis, and by matching the model heating value as closely as the true value. The optimum modelled composition of coal is summarised in Table I.

The rate of devolatilisation process was modeled using the first-order expression shown in equation 1:

$$\frac{dV}{dt} = k_1(V^* - V) \qquad (1a)$$

$$k_1 = k_{1,0}\exp\left(-E_1/RT_f\right), \qquad (1b)$$

where V is the volatile yield at time t, k_1 is the rate constant, V^* is the final volatile yield, T_f is the gas temperature, and, R is the gas constant. V^* was taken as 33.41%, based on the modelled coal composition given

in Table I. The Arrhenius parameters in equation 1b ($k_{1,0}=1.14\text{x}10^7$ s^{-1} and $E_1=74.5$ kJ/mol）were taken from Badzioch and Hawksley [8].

2.3 Gas-phase combustion

In the presence of oxygen (for cases where there is insufficient solar radiation to heat the reactor to the required temperature), the combustion of combustible gases occurs via reactions R2-R5.

$$H_2 + \frac{1}{2}O_2 \rightarrow H_2O \qquad (R2)$$

$$CH_4 + 2O_2 \rightarrow CO_2 + 2H_2O \qquad (R3)$$

$$CO + \frac{1}{2}O_2 \rightarrow CO_2 . \qquad (R4)$$

Here, these reactions are assumed to occur fast enough, in the presence of oxygen, to be considered instantaneous. This assumption is justified since the gasification reactions occur considerably slower than the combustion reactions.

2.4 Char combustion and gasification

The unreacted-shrinking core model of Wen *et al.* [9] was used to model char combustion and gasification. This model considers ash layer diffusion, gas film diffusion and chemical reaction. The combustion of char in the presence of oxygen is given by R5:

$$C + \frac{1}{\phi}O_2 \rightarrow 2\left(1 - \frac{1}{\phi}\right)CO + \left(\frac{2}{\phi} - 1\right)CO_2 . \qquad (R5)$$
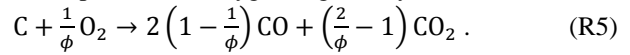
The mechanism factor, ϕ, is given by:

$$\phi = \left[(2Z + 2) - Z\left(d_p - 0.005\right)/0.095\right]/(Z + 2) \quad (5a)$$

where $Z = 2500\exp(-6249/T)$ and $T = \left(T_p + T_f\right)/2$. The rate of this reaction is given by:

$$R_5 = \frac{p_{o2}4\pi r_p^2}{\frac{1}{k_{5,diff}} + \frac{1}{k_{5,s}Y^2} + \frac{1}{k_{5,ash}\left(\frac{1}{Y}-1\right)}}, \qquad (5b)$$

where r_p is the particle radius, p_{O2} is the partial pressure of oxygen in the gasifier at residence time t, $k_{5,\text{diff}}$, $k_{5,s}$ and $k_{5,\text{ash}}$ are the surface diffusional, reaction and ash layer rate constants for reaction R5. Here Y is given by $[(1 - x)/(1 - f)]^{1/3}$, where f is the coal conversion at the end of the devolatilisation stage and x is the conversion at any time after this. The determination of all of these parameters is based on the work of Wen and Chaung [6].

Similarly, gasification occurs via reactions R6-R9.

$$C + H_2O \rightarrow CO + H_2 \qquad (R6)$$

$$C + CO_2 \rightarrow 2CO \qquad (R7)$$

$$C + 2H_2 \rightarrow CH_4 . \qquad (R8)$$

The determination of the rates of these reactions is based on the work of Wen and Chaung [6]:

$$R_6 = \frac{\left(p_{H_2O} - \frac{p_{H_2}p_{CO}}{k_{eq,6}}\right)4\pi r_p^2}{\frac{1}{k_{6,diff}} + \frac{1}{k_{6,s}Y^2} + \frac{1}{k_{6,ash}\left(\frac{1}{Y}-1\right)}} \qquad (6)$$

$$R_7 = \frac{p_{CO_2}4\pi r_p^2}{\frac{1}{k_{7,diff}} + \frac{1}{k_{7,s}Y^2} + \frac{1}{k_{7,ash}\left(\frac{1}{Y}-1\right)}} \qquad (7)$$

$$R_8 = \frac{\left(p_{H_2} - \sqrt{\frac{pCH_4}{k_{eq,8}}}\right)4\pi r_p^2}{\frac{1}{k_{8,diff}} + \frac{1}{k_{8,s}Y^2} + \frac{1}{k_{8,ash}\left(\frac{1}{Y}-1\right)}}, \qquad (8)$$

where p_{H2O}, p_{H2}, p_{CO}, p_{CO2}, p_{CH4} are the partial pressures of steam, hydrogen, carbon monoxide, carbon dioxide and methane in the gasifier at residence time t, $k_{i,\text{diff}}$, $k_{i,s}$

and $k_{i,ash}$ are the surface diffusional, reaction and ash layer rate constants for reaction Ri (where i=6-9). The determination of all these parameters is again based on the work of Wen and Chaung [6]. The total rate of char reaction due to combustion and gasification is hence given by:

$$\dot{m}_c = R_5 + R_6 + R_7 + R_8 . \tag{9}$$

2.5 Other gas-phase reactions

The homogenous gas phase reactions of importance to gasification are the water gas shift reaction (R10) and the methane reforming reaction (R11).

$$CO + H_2O \leftrightarrow CO_2 + H_2 \tag{R10}$$
$$CH_4 + H_2O \leftrightarrow CO + 3H_2 . \tag{R11}$$
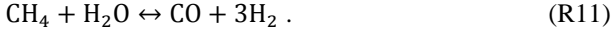
The rates of these reactions are given by equations 10 and 11. For both reactions the rate constants for the forward reactions were taken from Jones and Linstedt [10] and, for the water gas shift reaction, the equilibrium constant, $K_{eq,10}$, was determined from the Gibbs free energy change for reaction R10.

$$R_{10} = k_{10,0}\exp\left(-\frac{E_{10}}{RT_f}\right)$$
$$\times \left([CO][H_2O] - [CO_2][H_2]/K_{eq,10}\right) \tag{10}$$
$$R_{11} = k_{11,0}\exp\left(-E_{11}/RT_f\right)\left([CH_4][H_2O]\right) . \tag{11}$$

2.6 Heat Transfer

Modelling of heat transfer in the gasifier was based on the long furnace model used in previous studies of Wen and Chaung [6] and Govind and Shah [7]. The traditional long furnace model assumes are that no heat transfer occurs axially along the reactor, thus implying that radiant energy emitted in each slice is absorbed within the same slice. For this study, the traditional long furnace model is adapted slightly to allow solar radiation to pass axially along the reactor, although all other forms of heat were assumed to be absorbed within the gases, particles and walls of the individual slice. Additionally, all surfaces (particles and walls) are considered grey surfaces for radiation, and the gas phase is not regarded as a participating gas to radiation heat transfer.

The coal particles undergo heating via solar radiation (when present), char combustion (when oxygen is present) as well as convective heat transfer to the gases and radiative heat transfer from the hot walls. The endothermic gasification reactions were also taken into account. Thus,

$$\rho_p c_{p,p} V_p \frac{dT_p}{dt} = Q_{solar} + Q_{char\ combust}$$
$$-Q_{gasif} - Q_{pf} - Q_{pw} , \tag{12}$$

where T_p is the particle temperature, ρ_p is the particle density, $c_{p,p}$ is the particle's specific heat and V_p is the particle volume. The terms on the right-hand side are given by equations 13-17:

$$Q_{solar} = \pi r_p^2 \varepsilon_p I_{sol}(exp(-Ax)) \tag{13}$$
$$Q_{char\ combust} = \Delta H_5 R_5 \tag{14}$$
$$Q_{gasif} = \Delta H_6 R_6 + \Delta H_7 R_7 + \Delta H_8 R_8 \tag{15}$$
$$Q_{pw} = 4\pi r_p^2 \varepsilon_p \sigma\left(T_p^4 - T_w^4\right) \tag{16}$$
$$Q_{pf} = h_{pf} 4\pi r_p^2\left(T_p - T_f\right) , \tag{17}$$

where ε_p is the particle emissivity (assumed 0.9), A is the absorbtivity of the solar radiation by the particles (calculated as a function of particle loading based on the

work of Z'Graggen et al [5]), I_{sol} is the input solar flux (maximum of 4 MW/m^2), x is the axial distance along the reactor, T_f is the gas temperature, T_w is the wall temperature (assumed to be 1700K based on Z'Graggen et al [4]), h_{pf} is the convective heat transfer coefficient between the solid particle and the gases, σ is the Stefan-Boltzmann constant, and ΔH_i, is the enthalpy of reaction i (where i=5-9).

Similarly, the components of heat transfer to the gases in the reactor comprise the combustion of the volatiles (when oxygen is present), enthalpy change due to the water-gas shift and methane reforming reactions and heat exchange of the gas with particles and the reactor walls. Thus,

$$\rho_f c_{p,f} V_f \frac{dT_f}{dt} = Q_{vol\ combust} + Q_{wgs} - Q_{mr}$$
$$+ N.Q_{pf} - Q_{fw} \tag{18}$$
$$Q_{vol\ combust} = \Delta H_{vol\ combust}\dot{m}_{vol\ released} \tag{19}$$
$$Q_{wgs} = \Delta H_{wgs} R_8 V_f \tag{20}$$
$$Q_{mr} = \Delta H_{mr} R_9 V_f \tag{21}$$
$$Q_{fw} = h_{fw} A_w\left(T_f - T_w\right) , \tag{22}$$

where ε_w is the wall emissivity (assumed 0.78), ρ_f is the gas density, $c_{p,f}$ is the gas specific heat, V_f is the volume of the gases in the modelled region, N is the number of particles within the modelled region, A_w is the surface area of the wall within the modelled region, h_{fw} is the convective heat transfer coefficient between the gases and the reactor wall, $\dot{m}_{vol\ released}$ is the rate of mass loss of volatiles at time t, $\Delta H_{vol\ combust}$ is the enthalpy of combustion of the volatiles and ΔH_i, is the enthalpy change of reaction i (where i=10-11).

Drying of coal particles in the gasifier was assumed to be limited by heat transfer to the particle. The particle was assumed to heat up to 373K by heat from walls, hot gases and solar radiation (if available), after which moisture is evaporated at a rate dependent on the particle heating rate. While the particle moisture content is greater than zero, the moisture loss model, is given by:

$$\dot{m}_{H2O} = -Q_{particle}/\Delta H_{evap} , \tag{23}$$

where, $\dot{m}_{H2O}$ is the rate of mass loss of moisture from the particle at time t, ΔH_{evap} is the enthalpy of evaporation of water and $Q_{particle}$ is the total heating rate of the particle at a given time.

3. Results

Typical results obtained from the model are shown in Figures 2-5 for the two cases of (i) fully autothermal gasification (ie. $Q_{solar} = 0$, Oxygen/Fuel (O/F) = 0.9 and Steam/Fuel (S/F) = 0.1), and, (ii) fully solar gasification for $Q_{solar} = 4$ MW/m^2 (O/F = 0, S/F = 1). Figure 2 shows the temperature of the gas and solid particles for the autothermal case. Both gas and particle temperatures quickly reach their respective peak within less than 100ms of the inlet of the reactor, primarily due to the combustion of volatiles. Figure 3 shows that during this initial 100ms the CO_2 and H_2O concentrations increase due to the presence of oxygen, and then decrease slowly to about a quarter of their initial value as they are consumed by the gasification reactions. During the

reactions, the concentrations of both H_2 and CO increase monotonically, and do not stabilize within the residence time of the reactor. At the exit of the reactor (4s) the coal conversion is ~95% and the H_2/CO ratio is 0.37. The total residence time utilised in this study is similar to that of industrial scale entrained flow gasifiers which are typically 0.5-4 s [11].

Figure 4 shows the temperature of the gas and solid particles for the solar case. Both gas and particle temperatures reach their respective peaks within 400ms of the inlet of the reactor, due to the solar radiation. Figure 5 shows that, during the initial 200ms, the CH_4 concentration is substantial due to the absence of oxygen. However, after this time the CH_4 is consumed by the methane reforming reaction (R11). At the exit of the reactor the coal conversion is ~95% and the H_2/CO ratio is 1.5. The CO_2 concentration of the syngas is also quite low compared with the autothermal case (2% vs 7% at the exit). For a hybrid process, these large differences in gas compositions represents a challenge, since the commercially available processes to convert syngas to liquid fuels require a consistent feed and composition of syngas. Hence, syngas storage will be required for a plant operating with a hybrid solar/oxygen entrained-flow gasifier to counteract this problem, as suggested by Kaniyal et al. [12].
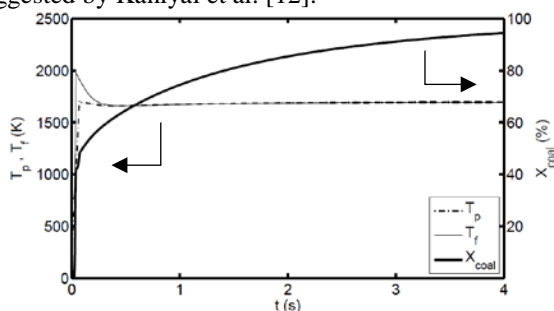

Figure 2: Temperature and coal conversion profiles plotted against residence time for O/F=0.9, S/F=0.1, 0 MW/m² input solar.
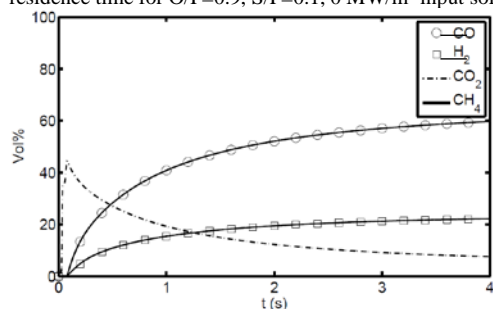

Figure 3: Gas composition profiles plotted against residence time along the reactor for O/F=0.9, S/F=0.1, 0 MW/m² input solar.
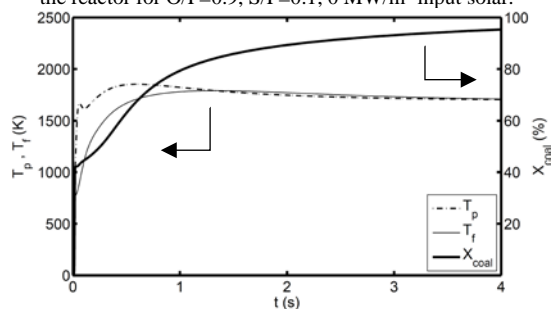

Figure 4: Temperature and coal conversion profiles plotted against residence time for O/F=0.0, S/F=1.0, 4 MW/m² input solar.
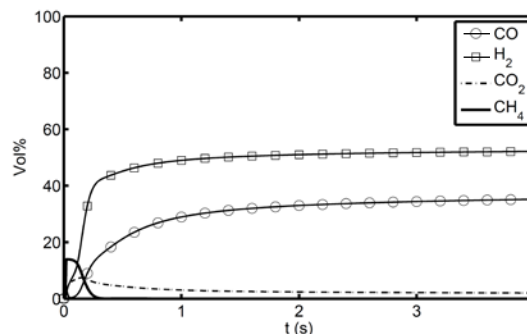

Figure 5: Gas composition profiles plotted against residence time along the reactor for O/F=0.0, S/F=1.0, 4 MW/m² input solar.

4. Conclusions

A mathematical model of a hybrid solar entrained-flow gasifier is presented. Calculations using this model predict that solar gasification of Illinois 6 coal during peak sun will result in similar coal conversions (~95%) and higher H_2/CO ratios (1.5 cf 0.37) relative to autothermal gasification. The CO_2 concentration of the syngas is also quite low compared to the autothermal case (2% cf 7% at the exit). Due to these large differences in outlet composition, it is apparent that syngas storage will be necessary for a coal to liquids plant with a hybrid solar/oxygen entrained-flow gasifier.

5. Acknowledgments

6. References

[1] T. Kodama. Prog. Energy and Combust. Sci. **29** (2003) 567-97.

[2] C. Wieckert, A. Obrist, P. von Zedtwitz, G. Maag, A. Steinfeld. Energy Fuels **27** (2013) 4770−4776.

[3] T. Kodama, T. Kondoh, T. Tamagawa, A. Funatoh, K.-I. Shimizu, Y. Kitayama. Energy Fuels **16** (2002) 1264-1270.

[4] A. Z'Graggen, P. Haueter, G. Maag, A. Vidal, M. Romero, A. Steinfeld. Int J Hyd Energy. **32** (2007) 992-996.

[5] A. Z'Graggen, A. Steinfeld. Int J Heat Mass Trans. **52** (2009) 385-95.

[6] C.Y. Wen and T.Z. Chaung, Ind. Eng. Chem. Process Des. Develop. **18** (1979) 684-695.

[7] R. Govind and J. Shah. AIChE J. **30** (1984) 79.

[8] S. Badzioch, P.B.W. Hawksley, Ind. Eng. Chem. Process Des. Develop. **9** (1970) 521-530.

[9] C.Y. Wen, Ind. Eng. Chem. **60** (1968) 34.

[10] W.P. Jones, R.P. Lindstedt, Combust. Flame 73 (1988) 233-249.

[11] C. Higman, M. van der Burg. Gasification. 2nd ed. ed. Oxford, UK: Elsevier; 2008.

[12] A. Kaniyal, P.J. van Eyk, G.J. Nathan, P.J. Ashman, J. Pincus. Energy Fuels **27** (2013) 3538-3555.